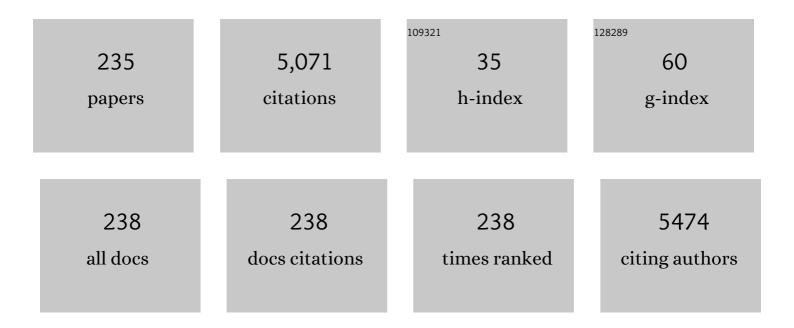
Eiichiro Matsubara

List of Publications by Year in descending order

Source: https://exaly.com/author-pdf/4577304/publications.pdf Version: 2024-02-01



#	Article	IF	CITATIONS
1	Excess free volume in metallic glasses measured by X-ray diffraction. Acta Materialia, 2005, 53, 1611-1619.	7.9	344
2	Direct Observation of a Metastable Crystal Phase of Li _{<i>x</i>} FePO ₄ under Electrochemical Phase Transition. Journal of the American Chemical Society, 2013, 135, 5497-5500.	13.7	177
3	Intercalation and Pushâ€Out Process with Spinelâ€ŧoâ€Rocksalt Transition on Mg Insertion into Spinel Oxides in Magnesium Batteries. Advanced Science, 2015, 2, 1500072.	11.2	153
4	Processing Pure Ti by High-Pressure Torsion in Wide Ranges of Pressures and Strain. Metallurgical and Materials Transactions A: Physical Metallurgy and Materials Science, 2009, 40, 2079-2086.	2.2	149
5	Hydrogen permeation and structural features of melt-spun Ni–Nb–Zr amorphous alloys. Acta Materialia, 2005, 53, 3703-3711.	7.9	134
6	A concept of dual-salt polyvalent-metal storage battery. Journal of Materials Chemistry A, 2014, 2, 1144-1149.	10.3	133
7	Transient Phase Change in Two Phase Reaction between LiFePO ₄ and FePO ₄ under Battery Operation. Chemistry of Materials, 2013, 25, 1032-1039.	6.7	122
8	Allotropic phase transformation of pure zirconium by high-pressure torsion. Materials Science & Engineering A: Structural Materials: Properties, Microstructure and Processing, 2009, 523, 277-281.	5.6	105
9	Electrochemical Stability of Magnesium Battery Current Collectors in a Grignard Reagent-Based Electrolyte. Journal of the Electrochemical Society, 2013, 160, C83-C88.	2.9	105
10	Crystallization Behavior of Amorphous Fe _{90−<i>X</i>} Nb ₁₀ B <i><sub& (<i>X</i>=10 and 30) Alloys. Materials Transactions, JIM, 2000, 41, 1526-1529.</sub& </i>	gt;XX&dt/Sl	JB &gz ,</l&g
11	Amorphous Metal Polysulfides: Electrode Materials with Unique Insertion/Extraction Reactions. Journal of the American Chemical Society, 2017, 139, 8796-8799.	13.7	84
12	Surface modification of ACM522 magnesium alloy by plasma electrolytic oxidation in phosphate electrolyte. Corrosion Science, 2012, 57, 74-80.	6.6	80
13	Toward "rocking-chair type―Mg–Li dual-salt batteries. Journal of Materials Chemistry A, 2015, 3, 10188-10194.	10.3	72
14	Direct observation of layered-to-spinel phase transformation in Li ₂ MnO ₃ and the spinel structure stabilised after the activation process. Journal of Materials Chemistry A, 2017, 5, 6695-6707.	10.3	72
15	Factors determining the packing-limitation of active materials in the composite electrode of lithium-ion batteries. Journal of Power Sources, 2016, 301, 11-17.	7.8	65
16	Three-Dimensional Electron Density Mapping of Shape-Controlled Nanoparticle by Focused Hard X-ray Diffraction Microscopy. Nano Letters, 2010, 10, 1922-1926.	9.1	63
17	Preferential formation of anatase in laser-ablated titanium dioxide films. Acta Materialia, 2005, 53, 323-329.	7.9	62
18	Ultrasound-induced crystallization around the glass transition temperature for Pd40Ni40P20 metallic glass. Acta Materialia. 2004. 52. 423-429.	7.9	61

#	Article	IF	CITATIONS
19	Stabilité de l'état vitreux dans des verres métalliques à bse de zirconium et corrélation avec la formation d'une phase icosaédrique nanométrique. Annales De Chimie: Science Des Materiaux, 2002, 27, 77-89.	0.4	60
20	High-resolution diffraction microscopy using the plane-wave field of a nearly diffraction limited focused x-ray beam. Physical Review B, 2009, 80, .	3.2	59
21	Formation of self-repairing anodized film on ACM522 magnesium alloy by plasma electrolytic oxidation. Corrosion Science, 2013, 73, 188-195.	6.6	55
22	Control of compound forming reaction at the interface between SnZn solder and Cu substrate. Journal of Alloys and Compounds, 2005, 392, 200-205.	5.5	54
23	Glass-liquid transition in a less-stable metallic glass. Physical Review B, 2005, 72, .	3.2	53
24	Phase Transition Analysis between LiFePO ₄ and FePO ₄ by In-Situ Time-Resolved X-ray Absorption and X-ray Diffraction. Journal of the Electrochemical Society, 2013, 160, A3061-A3065.	2.9	50
25	Three-Dimensional Nanoelectrode by Metal Nanowire Nonwoven Clothes. Nano Letters, 2014, 14, 1932-1937.	9.1	48
26	EQCM Analysis of Redox Behavior of CuFe Prussian Blue Analog in Mg Battery Electrolytes. Journal of the Electrochemical Society, 2015, 162, A2356-A2361.	2.9	48
27	Effect of Al on Local Structures of Zr–Ni and Zr–Cu Metallic Glasses. Materials Transactions, 2005, 46, 2893-2897.	1.2	46
28	Initial Atomic Motion Immediately Following Femtosecond-Laser Excitation in Phase-Change Materials. Physical Review Letters, 2016, 117, 135501.	7.8	45
29	Surface-layer formation by reductive decomposition of LiPF6 at relatively high potentials on negative electrodes in lithium ion batteries and its suppression. Journal of Power Sources, 2014, 271, 431-436.	7.8	43
30	Nanoquasicrystallization in Metallic Glasses. Materials Transactions, 2003, 44, 1971-1977.	1.2	40
31	High-resolution projection image reconstruction of thick objects by hard x-ray diffraction microscopy. Physical Review B, 2010, 82, .	3.2	38
32	<i>In-situ</i> X-ray Diffraction of Corrosion Products Formed on Iron Surfaces. Materials Transactions, 2005, 46, 637-642.	1.2	37
33	Mechanism of nanocrystalline microstructure formation in amorphousFeâ^'Nbâ^'Balloys. Physical Review B, 2006, 74, .	3.2	37
34	Electronic States of Sulfur Doped TiO ₂ by First Principles Calculations. Materials Transactions, 2004, 45, 1987-1990.	1.2	36
35	Synthesis of Binary Magnesium–Transition Metal Oxides via Inverse Coprecipitation. Japanese Journal of Applied Physics, 2013, 52, 025501.	1.5	36
36	Determination of Mo(VI) Species and Composition in Ni-Mo Alloy Plating Baths by Raman Spectra Factor Analysis. Journal of the Electrochemical Society, 2000, 147, 2210.	2.9	35

#	Article	IF	CITATIONS
37	One-pot synthesis of silica-coated copper nanoparticles with high chemical and thermal stability. Journal of Colloid and Interface Science, 2015, 460, 47-54.	9.4	35
38	Local Structure of Ferric Hydroxide Fe(OH) ₃ in Aqueous Solution by the Anomalous X-ray Scattering and EXAFS Methods. Materials Transactions, JIM, 1994, 35, 394-398.	0.9	34
39	Formation of Cu Nanoparticles by Electroless Deposition Using Aqueous CuO Suspension. Journal of the Electrochemical Society, 2008, 155, D474.	2.9	34
40	EQCM analysis of redox behavior of Prussian blue in a lithium battery electrolyte. Journal of Materials Chemistry A, 2014, 2, 8041.	10.3	34
41	Synthesis of Spinel-Type Magnesium Cobalt Oxide and Its Electrical Conductivity. Materials Transactions, 2008, 49, 824-828.	1.2	32
42	Partial structure analysis of amorphous Ge15Te80M5 (M=Cu, Ag and In). Journal of Non-Crystalline Solids, 2002, 312-314, 585-588.	3.1	31
43	Ex-situ and in-situ X-ray diffractions of corrosion products freshly formed on the surface of an iron–silicon alloy. Corrosion Science, 2007, 49, 1081-1096.	6.6	31
44	A new aspect of Chevrel compounds as positive electrodes for magnesium batteries. Journal of Materials Chemistry A, 2014, 2, 14858-14866.	10.3	31
45	Spectroscopic X-ray Diffraction for Microfocus Inspection of Li-Ion Batteries. Journal of Physical Chemistry C, 2014, 118, 20750-20755.	3.1	31
46	Constructing metal-anode rechargeable batteries utilizing concomitant intercalation of Li–Mg dual cations into Mo ₆ S ₈ . Journal of Materials Chemistry A, 2017, 5, 3534-3540.	10.3	30
47	Element-specific hard x-ray diffraction microscopy. Physical Review B, 2008, 78, .	3.2	29
48	Thickness estimation of interface films formed on Li1â^'xCoO2 electrodes by hard X-ray photoelectron spectroscopy. Journal of Power Sources, 2011, 196, 10679-10685.	7.8	29
49	Inhibition of Conversion Process from Fe(OH)3 to .BETAFeOOH and .ALPHAFe2O3 by the Addition of Silicate Ions. ISIJ International, 2005, 45, 77-81.	1.4	28
50	High oxide-ion conductivity of monovalent-metal-doped bismuth vanadate at intermediate temperatures. Solid State Ionics, 2010, 181, 719-723.	2.7	28
51	Mechanical synthesis and structural properties of the fast fluoride-ion conductor PbSnF4. Journal of Solid State Chemistry, 2017, 253, 287-293.	2.9	28
52	Intermediate-range order in glassy GexSe1â^'x around the stiffness transition composition. Journal of Non-Crystalline Solids, 2004, 337, 54-61.	3.1	27
53	Formation of Nickel Nanowires via Electroless Deposition Under a Magnetic Field. Journal of the Electrochemical Society, 2011, 158, E79.	2.9	27
54	Influence of Mechanical Strain on the Electrochemical Lithiation of Aluminum-Based Electrode Materials. Journal of the Electrochemical Society, 2011, 159, A14-A17.	2.9	27

#	Article	IF	CITATIONS
55	Roles of transition metals interchanging with lithium in electrode materials. Physical Chemistry Chemical Physics, 2015, 17, 14064-14070.	2.8	27
56	Approach for three-dimensional observation of mesoscopic precipitates in alloys by coherent x-ray diffraction microscopy. Applied Physics Letters, 2007, 90, 184105.	3.3	26
57	Fabrication of Cobalt Nanowires by Electroless Deposition under External Magnetic Field. Journal of the Electrochemical Society, 2011, 158, D210.	2.9	26
58	Elastically constrained phase-separation dynamics competing with the charge process in the LiFePO4/FePO4 system. Journal of Materials Chemistry A, 2013, 1, 2567.	10.3	26
59	Structural study in amorphous Zr–noble metal (Pd, Pt and Au) alloys. Journal of Non-Crystalline Solids, 2002, 312-314, 517-521.	3.1	25
60	Hidden Two-Step Phase Transition and Competing Reaction Pathways in LiFePO ₄ . Chemistry of Materials, 2017, 29, 2855-2863.	6.7	25
61	Local Structure and Glass Transition in Zr-Based Binary Amorphous Alloys. Materials Transactions, 2005, 46, 2282-2286.	1.2	24
62	Oxidation-State Control of Nanoparticles Synthesized via Chemical Reduction Using Potential Diagrams. Journal of the Electrochemical Society, 2009, 156, D321.	2.9	24
63	Effects of water content on magnesium deposition from a Grignard reagent-based tetrahydrofuran electrolyte. Research on Chemical Intermediates, 2014, 40, 3-9.	2.7	24
64	Electroless Deposition of Ferromagnetic Cobalt Nanoparticles in Propylene Glycol. Journal of the Electrochemical Society, 2009, 156, E139.	2.9	23
65	Nickel Alloying Effect on Formation of Cobalt Nanoparticles and Nanowires via Electroless Deposition under a Magnetic Field. Journal of the Electrochemical Society, 2011, 159, E37-E44.	2.9	23
66	Determination of Chemical Species and Their Composition in Niâ€Mo Alloy Plating Baths by Factor Analysis of Visible Absorption Spectra. Journal of the Electrochemical Society, 1998, 145, 523-528.	2.9	22
67	Effect of Silicate Ions on Conversion of Ferric Hydroxide to β-FeOOH and α-Fe ₂ O ₃ . Materials Transactions, 2005, 46, 155-158.	1.2	22
68	X-ray absorption fine-structure study on the fine structure of lutetium segregated at grain boundaries in fine-grained polycrystalline alumina. Philosophical Magazine, 2004, 84, 865-876.	1.6	21
69	Electrochemical Behavior of Magnesium Alloys in Alkali Metal-TFSA Ionic Liquid for Magnesium-Battery Negative Electrode. Journal of the Electrochemical Society, 2014, 161, A943-A947.	2.9	21
70	A Reversible Rocksalt to Amorphous Phase Transition Involving Anion Redox. Scientific Reports, 2018, 8, 15086.	3.3	21
71	Structural characterization of an amorphous VS ₄ and its lithiation/delithiation behavior studied by solid-state NMR spectroscopy. RSC Advances, 2019, 9, 23979-23985.	3.6	21
72	Characterization of Oxide Film Grown on Stainless Steel by a New In-House Grazing Incidence X-ray Scattering (GIXS) Apparatus. Materials Transactions, JIM, 1995, 36, 1-5.	0.9	20

#	Article	IF	CITATIONS
73	Epitaxial relation and island growth of perylene-3.4.9.10-tetracarboxylic dianhydride (PTCDA) thin film crystals on a hydrogen-terminated Si(111) substrate. Journal of Crystal Growth, 2004, 262, 196-201.	1.5	20
74	Local Atomic Structures of Amorphous Fe ₈₀ B ₂₀ and Fe ₇₀ Nb ₁₀ 8 ₂₀ Alloys Studied by Electron Diffraction. Materials Transactions, 2005, 46, 2781-2784.	1.2	20
75	Crystallization Behavior and Structural Stability of Zr ₅₀ Cu ₄₀ Al ₁₀ Bulk Metallic Glass. Materials Transactions, 2009, 50, 1340-1345.	1.2	20
76	Electrochemical Study on the Synthesis Process of Co–Ni Alloy Nanoparticles via Electroless Deposition. Journal of the Electrochemical Society, 2010, 157, E92.	2.9	20
77	Time-Resolved Coherent Diffraction of Ultrafast Structural Dynamics in a Single Nanowire. Nano Letters, 2014, 14, 2413-2418.	9.1	20
78	Structural Study of Liquid Na–Pb Alloys by Neutron Diffraction. Journal of the Physical Society of Japan, 1987, 56, 3934-3940.	1.6	19
79	Structural Study of Amorphous FE ₇₀ M ₁₀ B ₂₀ (M=CR, W, NB, ZR) Tj	ETQq1 1 0	0.784314 rg <mark>81</mark> 19
80	On the preferential formation of anatase in amorphous titanium oxide film. Scripta Materialia, 2005, 53, 1019-1023.	5.2	19
81	Analysis of the discharge/charge mechanism in VS4 positive electrode material. Solid State Ionics, 2018, 323, 32-36.	2.7	19
82	Two-Phase Reaction Mechanism for Fluorination and Defluorination in Fluoride-Shuttle Batteries: A First-Principles Study. ACS Applied Materials & Interfaces, 2020, 12, 428-435.	8.0	19
83	Precipitation of the ZrCu <i>B2</i> phase in Zr ₅₀ Cu _{50–} <i>_x</i> Al <i>_x</i> (si>x = 0, 4, 6) metallic glasses by rapidly heating and cooling. Journal of Materials Research, 2010, 25, 793-800.	2.6	18
84	Room-Temperature Synthesis of Cobalt Nanoparticles by Electroless Deposition in Aqueous Solution. Electrochemical and Solid-State Letters, 2010, 13, D4.	2.2	18
85	<i>In situ</i> two-dimensional imaging quick-scanning XAFS with pixel array detector. Journal of Synchrotron Radiation, 2011, 18, 919-922.	2.4	18
86	What determines the critical size for phase separation in LiFePO4 in lithium ion batteries?. Journal of Materials Chemistry A, 2013, 1, 14532.	10.3	18
87	Sequential delithiation behavior and structural rearrangement of a nanoscale composite-structured Li1.2Ni0.2Mn0.6O2 during charge–discharge cycles. Scientific Reports, 2020, 10, 10048.	3.3	18
88	Crystallisation behaviour of Cu60Zr30Ti10 bulk glassy alloy. Materials Science & Engineering A: Structural Materials: Properties, Microstructure and Processing, 2004, 375-377, 744-748.	5.6	17
89	Viscosity of glassy Na2O- B2O2 SiO2 system. Journal of Non-Crystalline Solids, 1987, 95-96, 1031-1038.	3.1	16
90	Determination of Atomic Sites of Nb Dissolved in Metastable Fe ₂₃ B ₆ Phase. Materials Transactions, 2002, 43, 1918-1920.	1.2	16

#	Article	IF	CITATIONS
91	Local Atomic Structure and Catalytic Activities in Electrodeposited Mo-Ni Alloys. Materials Transactions, 2002, 43, 1525-1529.	1.2	16
92	Elemental identification of a three-dimensional environment by complex x-ray holography. Physical Review B, 2005, 71, .	3.2	16
93	Reaction Mechanism of Li ₂ MnO ₃ Electrodes in an All-Solid-State Thin-Film Battery Analyzed by Operando Hard X-ray Photoelectron Spectroscopy. Journal of the American Chemical Society, 2022, 144, 236-247.	13.7	16
94	Anomalous Grazing X-ray Reflectometry for Determining the Number Density of Atoms in the Near-Surface Region. Materials Transactions, JIM, 1996, 37, 39-44.	0.9	15
95	Formation of Nickel Nanoparticles by Electroless Deposition Using NiO and Ni(OH)[sub 2] Suspensions. Journal of the Electrochemical Society, 2008, 155, D583.	2.9	15
96	Electrochemical QCM Study of the Synthesis Process of Cobalt Nanoparticles via Electroless Deposition. Electrochemical and Solid-State Letters, 2010, 13, E1.	2.2	15
97	Electroless Deposition of Cobalt Nanowires in an Aqueous Solution under External Magnetic Field. Electrochemical and Solid-State Letters, 2011, 14, D68.	2.2	15
98	Quantitative Analysis of Transition-Metal Migration Induced Electrochemically in Lithium-Rich Layered Oxide Cathode and Its Contribution to Properties at High and Low Temperatures. Journal of Physical Chemistry C, 2016, 120, 27109-27116.	3.1	15
99	Characterization of the Ni-Zn/TiO ₂ Nanocomposite Synthesized by the Liquid-Phase Selective-Deposition Method. Materials Transactions, 2004, 45, 2035-2038.	1.2	14
100	Structure of Bis(iodozincio)methane in THF Solution. Chemistry Letters, 2005, 34, 952-953.	1.3	14
101	Atomic imaging in EBCO superconductor films by an X-ray holography system using a toroidally bent graphite analyzer. Journal of Synchrotron Radiation, 2005, 12, 530-533.	2.4	14
102	Revisit to diffraction anomalous fine structure. Journal of Synchrotron Radiation, 2014, 21, 1247-1251.	2.4	14
103	Strain-Induced Stabilization of Charged State in Li-Rich Layered Transition-Metal Oxide for Lithium-Ion Batteries. Journal of Physical Chemistry C, 2018, 122, 19298-19308.	3.1	14
104	Analysis of Cathode Reactions of Lithium Ion Cells Using Dynamic Electrochemical Impedance. Journal of the Electrochemical Society, 2020, 167, 020502.	2.9	14
105	A New Quantitative Anomalous X-ray Scattering Method for the Structural Analysis of Amorphous Thin Films. Transactions of the Japan Institute of Metals, 1988, 29, 697-704.	0.5	13
106	Structure and reactivity of bis(iodozincio)methane solution. Journal of Organometallic Chemistry, 2005, 690, 5546-5551.	1.8	13
107	Correlation between local structure and stability of supercooled liquid state in Zr-based metallic glasses. Materials Science & Engineering A: Structural Materials: Properties, Microstructure and Processing, 2007, 449-451, 90-94.	5.6	13
108	X-ray Fluorescence Holography Study on Si _{1−} <i>_x</i> Ge <i>_x</i> Single Crystal. Materials Transactions, 2004, 45, 1994-1997.	1.2	12

#	Article	IF	CITATIONS
109	Three-Dimensional Atomic Image around Mn Atoms in Diluted Magnetic Semiconductor Zn0.4Mn0.6Te Obtained by X-Ray Fluorescence Holography. Japanese Journal of Applied Physics, 2005, 44, 1011-1012.	1.5	12
110	Application of x-ray excited optical luminescence to x-ray standing wave method and atomic resolution holography. Physical Review B, 2007, 76, .	3.2	12
111	Effect of relaxation state on nucleation and grain growth of nanoscale quasicrystal in Zr-based bulk metallic glasses prepared under various cooling rates. Applied Physics Letters, 2011, 99, 061903.	3.3	12
112	Kinetically asymmetric charge and discharge behavior of LiNi0.5Mn1.5O4 at low temperature observed by in situ X-ray diffraction. Journal of Materials Chemistry A, 2014, 2, 15414-15419.	10.3	12
113	Effects of Film Formation on the Electrodeposition of Lithium. ChemElectroChem, 2020, 7, 4336-4342.	3.4	12
114	Atomic Structure Analysis of Amorphous Tb-Fe1-xCoxFilm Systems. Japanese Journal of Applied Physics, 1991, 30, 764-767.	1.5	11
115	Anomalous X-ray Scattering Study of Local Structures in the Superionic Conducting Glass (CuI) _{0.3} (Cu ₂ O) _{0.35} (MoO <sub> Materials Transactions, JIM, 1995, 36, 1434-1439.</sub> 	;3 &l g/SUE	3&g t ;)<SUE
116	Local structure in quasicrystal-forming Zr-based metallic glasses correlated with a stability of the supercooled liquid state. Journal of Non-Crystalline Solids, 2007, 353, 3704-3708.	3.1	11
117	Glass-to-liquid transition in zirconium and palladium based metallic glasses. Materials Science & Engineering A: Structural Materials: Properties, Microstructure and Processing, 2007, 449-451, 506-510.	5.6	11
118	A Pseudoternary Phase Diagram of the BaO-ZrO2-ScO1.5 System at 1600°C and Solubility of Scandia into Barium Zirconate. Journal of Phase Equilibria and Diffusion, 2007, 28, 517-522.	1.4	11
119	Structural Analysis of Pd-Cu-Si Metallic Glassy Alloy Thin Films with Varying Glass Transition Temperature. Materials Transactions, 2011, 52, 1349-1355.	1.2	11
120	Structure analyses of Fe-substituted Li2S-based positive electrode materials for Li-S batteries. Solid State Ionics, 2018, 320, 387-391.	2.7	11
121	Operando analysis of electronic band structure in an all-solid-state thin-film battery. Communications Chemistry, 2022, 5, .	4.5	11
122	Development of laboratory x-ray fluorescence holography equipment. Journal of Materials Research, 2003, 18, 1471-1473.	2.6	10
123	Crystallization accelerated by ultrasound in Pd-based metallic glasses. Journal of Alloys and Compounds, 2007, 434-435, 194-195.	5.5	10
124	Phase classification, electrical conductivity, and thermal stability of Bi2(V0.95TM0.05)O5.5+δ (TM:) Tj ETQq0 0 C	rgBT /Ove	erlock 10 Tf 5
125	Effect of Composition and Microstructure of Pd-Cu-Si Metallic Glassy Alloy Thin Films on Hydrogen Absorbing Properties. Materials Transactions, 2011, 52, 1807-1813.	1.2	10

#	Article	IF	CITATIONS
127	Mechanism of Structural Change and the Trigger of Electrochemical Degradation of Li-Rich Layered Oxide Cathodes during Charge–Discharge Cycles. ACS Applied Energy Materials, 2019, 2, 8118-8124.	5.1	10
128	Structural study of liquid Naî—,Tl alloys by neutron diffraction. Journal of Non-Crystalline Solids, 1990, 117-118, 68-71.	3.1	9
129	Structural Study of Poly-Molybdate Ions in Acid Mo-Ni Aqueous Solutions. Zeitschrift Fur Naturforschung - Section A Journal of Physical Sciences, 1997, 52, 855-862.	1.5	9
130	Fullerene and Sulfur Compounds. Materials Transactions, 2002, 43, 1530-1532.	1.2	9
131	Incident Photon-Energy Dependence of the Electronic Density of States in Pd _{42.5} Ni _{7.5} Cu ₃₀ P ₂₀ Metallic Glass. Materials Transactions, 2005, 46, 2803-2806.	1.2	9
132	X-ray fluorescence holography of 0.078wt% copper in silicon steel. Nuclear Instruments & Methods in Physics Research B, 2005, 238, 192-195.	1.4	9
133	Crystallization behaviours around the glass transition temperature in an amorphous Fe–Nb–B alloy. Intermetallics, 2009, 17, 796-801.	3.9	9
134	Femtosecond Snapshot Holography with Extended Reference Using Extreme Ultraviolet Free-Electron Laser. Applied Physics Express, 2010, 3, 102701.	2.4	9
135	Structure and Hydrogen Permeation of Ni-Nb-Zr Amorphous Alloy. Journal of Metastable and Nanocrystalline Materials, 2005, 24-25, 551-554.	0.1	8
136	Reconstruction of atomic images from multiple-energy x-ray holograms of FePt films by the scattering pattern matrix method. Applied Physics Letters, 2005, 87, 234104.	3.3	8
137	Holographic Analysis of Incident Electron Beam Angular Distribution of Characteristic X-rays: Internal Detector Electron Holography. Journal of the Physical Society of Japan, 2006, 75, 053601.	1.6	8
138	Local Structure Study in Zr-Based Metallic Glasses. Materials Transactions, 2007, 48, 1703-1707.	1.2	8
139	Improvement of Cycle Capability of Fe-Substituted Li ₂ S-Based Positive Electrode Materials by Doping with Lithium Iodide. Journal of the Electrochemical Society, 2019, 166, A5231-A5236.	2.9	8
140	The Structure of Liquid Bi–Zn Alloys with Miscibility Gaps. Journal of the Physical Society of Japan, 1986, 55, 4296-4301.	1.6	7
141	Methods for the Quantitative Structural Analysis of Amorphous Ge Thin Film by X-rays. Transactions of the Japan Institute of Metals, 1988, 29, 1-7.	0.5	7
142	Preparation of a TiO ₂ Film Coated Si Device for Photo-Decomposition of Water by CVD Method Using Ti(OPr ⁱ) ₄ . Materials Transactions, 2002, 43, 1533-1536.	1.2	7
143	Evidence for the Diffusion of Au Atoms into the Te UPD Layer Formed on a Au(111) Substrate. Journal of the Electrochemical Society, 2002, 149, C83.	2.9	7
144	EXAFS and SAXS analysis for nano-structural origin of high strength for supersaturated Al100â^'Fe (x =) Tj ETQq0	0 0 rgBT / 5.6	Overlock 10 7

and Processing, 2004, 375-377, 1224-1227.

#	Article	IF	CITATIONS
145	Ultrasound-Induced Structural Anomaly of Supercooled Liquid in Some Bulk Metallic Glasses. Materials Transactions, 2004, 45, 1189-1193.	1.2	7
146	Formation of Tin Nanoparticles Embedded in Poly(L-Lactic Acid) Fiber by Electrospinning. Electrochemical and Solid-State Letters, 2008, 11, E25.	2.2	7
147	Abnormal Behavior of Hydrogen Response and Hydrogen Induced Linear Expansion Coefficient of Pd-Cu-Si Metallic Glassy Alloys for Thin Film Hydrogen Sensor. Materials Transactions, 2011, 52, 1148-1155.	1.2	7
148	Iron Alloying Effect on Formation of Cobalt Nanoparticles and Nanowires via Electroless Deposition under a Magnetic Field. Journal of the Electrochemical Society, 2014, 161, D59-D66.	2.9	7
149	Direct Synthesis of Carbon–Molybdenum Carbide Nanosheet Composites via a Pseudotopotactic Solid-State Reaction. Chemistry of Materials, 2016, 28, 8899-8904.	6.7	7
150	Site-Selective Analysis of Nickel-Substituted Li-Rich Layered Material: Migration and Role of Transition Metal at Charging and Discharging. Journal of Physical Chemistry C, 2018, 122, 20099-20107.	3.1	7
151	Surface Structure of Nanometer-Sized Zinc Ferrite Particles by the Anomalous X-ray Scattering (AXS) Method. Zeitschrift Fur Naturforschung - Section A Journal of Physical Sciences, 1992, 47, 1023-1028.	1.5	6
152	Observation of electromigration in a Cu thin line by in situ coherent x-ray diffraction microscopy. Journal of Applied Physics, 2009, 105, 124911.	2.5	6
153	Research Update: Retardation and acceleration of phase separation evaluated from observation of imbalance between structure and valence in LiFePO4/FePO4 electrode. APL Materials, 2014, 2, 070701.	5.1	6
154	Diffuse Scattering of Superionic Phase of Cu2Se. Journal of the Physical Society of Japan, 1993, 62, 3513-3518.	1.6	5
155	Magnetic properties of Fe-based icosahedral cluster amorphous alloys. Materials Science & Engineering A: Structural Materials: Properties, Microstructure and Processing, 1994, 181-182, 860-863.	5.6	5
156	Structural Study of Poly-Molybdate Ions in Acid Mo–Ni Aqueuous Solutions. Japanese Journal of Applied Physics, 1999, 38, 576.	1.5	5
157	Structural Study of Thin Amorphous SiO2 and Si3N4 Films by the Grazing Incidence X-Ray Scattering (GIXS) Method. High Temperature Materials and Processes, 1999, 18, 99-107.	1.4	5
158	Application of Energy Dispersive Grazing Incidence X-ray Reflectometry Method to Structural Analysis of Liquid/Liquid and Liquid/Solid Interfaces. Materials Transactions, JIM, 2000, 41, 1651-1656.	0.9	5
159	The crystal structure and electronic properties of a new metastable non-stoichiometric BaAl4-type compound crystallized from amorphous La6Ni34Ge6Oalloy. Journal of Physics Condensed Matter, 2004, 16, 7917-7930.	1.8	5
160	Crystallization Behavior of αFe in Fe ₈₄ Nb ₇ B ₉ and Fe ₈₅ Nb ₆ B ₉ Amorphous Alloys. Materials Transactions, 2004, 45, 1199-1203.	1.2	5
161	Local Structure around Pd Atoms in Pd _{42.5} Ni _{7.5} Cu ₃₀ P _{20Excellent Glass-Former Studied by Anomalous X-ray Scattering. Materials Transactions, 2007, 48, 2358-2361.}	SUB> 1.2	5
162	<i>In situ</i> structural analysis of corrosion products formed on the surfaces of ironâ€based alloys. Surface and Interface Analysis, 2008, 40, 307-310.	1.8	5

#	Article	IF	CITATIONS
163	Room-Temperature Synthesis of Cobalt Nanoparticles in Aqueous Solution. ECS Transactions, 2010, 28, 29-34.	0.5	5
164	High-capacity Lithium-ion Storage System Using Unilamellar Crystallites of Exfoliated MoO2 Nanosheets. Chemistry Letters, 2015, 44, 1595-1597.	1.3	5
165	Magnetic field strength controlled liquid phase syntheses of ferromagnetic metal nanowire. Nanotechnology, 2020, 31, 365602.	2.6	5
166	The Additional Effect of Zn to Ni Nanoparticles and Their Catalytic Activity Shigen-to-Sozai, 2002, 118, 211-216.	0.1	5
167	Local Atomic Structures of Zr ₇₀ Ga ₁₀ Ni ₂₀ Amorphous Alloys by the Anomalous X-ray Scattering Method. Materials Transactions, JIM, 1995, 36, 1093-1096.	0.9	4
168	Development of New In-House Grazing X-ray Reflection System for Analyzing Liquid Surface and Interface. Materials Transactions, JIM, 1996, 37, 1409-1412.	0.9	4
169	Structural Studies of Aqueous Solutions by the Anomalous X-ray Scattering Method. High Temperature Materials and Processes, 1998, 17, 133-143.	1.4	4
170	Toroidal Bend Graphite X-ray Monochomator Materia Japan, 1999, 38, 43-45.	0.1	4
171	Local Atomic Structure and Electronic State of ZnS Films Synthesized by Using CBD Technique. Materials Transactions, 2002, 43, 1512-1516.	1.2	4
172	Effect of Al on the local structure and stability of Zr-based metallic glasses. Journal of Alloys and Compounds, 2007, 434-435, 135-137.	5.5	4
173	Effects of oxygen content and heating rate on phase transition behavior in Bi2(V0.95Ti0.05)O5.475â^'x. Journal of Alloys and Compounds, 2011, 509, 5833-5838.	5.5	4
174	Contactless analysis of electric dipoles at high- <i>k</i> /SiO2 interfaces by surface-charge-switched electron spectroscopy. Applied Physics Letters, 2016, 108, .	3.3	4
175	Structural and dynamic behavior of lithium iron polysulfide Li 8 FeS 5 during charge–discharge cycling. Journal of Power Sources, 2018, 398, 67-74.	7.8	4
176	Degradation mechanisms of lithium sulfide (Li ₂ S) composite cathode in carbonate electrolyte and improvement by increasing electrolyte concentration. Sustainable Energy and Fuels, 2021, 5, 1714-1726.	4.9	4
177	Feasibility Study of Local Structure Analysis of Ultrathin Films by X-ray Fluorescence Holography. Materials Transactions, 2002, 43, 1475-1479.	1.2	3
178	Development of in-house fast X-ray diffraction apparatus and its application to the supercooled liquid Pd40Ni10Cu30P20alloy. Science and Technology of Advanced Materials, 2002, 3, 69-73.	6.1	3
179	Partial Sulfurization of Laser-ablated Titanium Oxide Film for the Improvement in Photocatalytic Property. Materials Transactions, 2003, 44, 685-687.	1.2	3
180	Study on Fabrication of Titanium Oxide Films by Oxygen Pressure Controlled Pulsed Laser Deposition. Materials Transactions, 2004, 45, 2068-2072.	1.2	3

#	Article	IF	CITATIONS
181	Suppression of the Conversion Process of Fe(OH)3 to β-FeOOH and α-Fe2O3 by Silicate lons. High Temperature Materials and Processes, 2005, 24, 275-288.	1.4	3
182	Atomizing Effect on Sn-Zn Based Solder Alloy. Nippon Kinzoku Gakkaishi/Journal of the Japan Institute of Metals, 2006, 70, 162-165.	0.4	3
183	Phase Stability of Bi ₂ (V _{1−<i>x</i>} ME <i>_x</i>)O _{5.5+δ} (ME=Li and Ag, <i>x</i> =0.05 and 0.1). Materials Transactions, 2010, 51, 561-566.	1.2	3
184	Change in local environment upon quasicrystallization of Zr–Cu glassy alloys by addition of Pd and Pt. Journal of Physics Condensed Matter, 2011, 23, 175303.	1.8	3
185	Electroless Deposition of Nickel Nanoparticles at Room Temperature. Advanced Materials Research, 0, 974, 107-111.	0.3	3
186	Synthesis of Silica-Coated Copper Nanoparticles and its Application to Red Color Glaze. Advanced Materials Research, 2014, 970, 288-292.	0.3	3
187	Structural modification by adding Li cations into Mg/Cs-TFSA molten salt facilitating Mg electrodeposition. RSC Advances, 2015, 5, 3063-3069.	3.6	3
188	Ligancy-Driven Controlling of Covalency and Metallicity in a Ruthenium Two-Dimensional System. Chemistry of Materials, 2016, 28, 5784-5790.	6.7	3
189	Site- and phase-selective x-ray absorption spectroscopy based on phase-retrieval calculation. Journal of Physics Condensed Matter, 2017, 29, 113002.	1.8	3
190	Direct observation of elastic softening immediately after femtosecond-laser excitation in a phase-change material. Physical Review B, 2020, 101, .	3.2	3
191	Crystallization of Zr50Cu40Al10 Metallic Class by Rapid Heating Process. Zairyo/Journal of the Society of Materials Science, Japan, 2009, 58, 205-208.	0.2	3
192	The Structure of Amorphous Platinum Disulfide as Studied by Anomalous X-ray Scattering. Zeitschrift Fur Naturforschung - Section A Journal of Physical Sciences, 1994, 49, 1031-1036.	1.5	2
193	Local Atomic Structures in Amorphous and Quasicrystalline Zr70Ni10Pt20and Zr80Pt20Alloys by the Anomalous X-ray Scattering Method. Materials Research Society Symposia Proceedings, 2000, 644, 111.	0.1	2
194	è›å‰Xç·šāf›āfā,°āf©āf•ā,£āf¼æŠ€è;"ā®ç¾çжã•ãã®å°†æ¥çš"展é−‹. Materia Japan, 2001, 40, 801-807.	0.1	2
195	In-house Anomalous X-ray Scattering Analysis for the Amorphous Zr ₆₀ Al ₁₅ Ni ₂₅ Alloy. Materials Transactions, 2001, 42, 1977-1980.	1.2	2
196	Anomalous Crystallization Induced by Ultrasound in Pd _{42.5} Ni _{7.5} Cu ₃₀ P ₂₀ Metallic Glass. Journal of Metastable and Nanocrystalline Materials, 2005, 24-25, 547-550.	0.1	2
197	Structural Stability and Elasticity in Zr-Based Bulk Metallic Glasses. Materials Science Forum, 2007, 561-565, 1391-1395.	0.3	2
198	Coherent xâ€ray diffraction measurements of Cu thin lines. Surface and Interface Analysis, 2008, 40, 1046-1049.	1.8	2

#	Article	IF	CITATIONS
199	Growth of Cobalt Nanowires under External Magnetic Field. Advanced Materials Research, 0, 911, 136-140.	0.3	2
200	Liquid-phase synthesis of Ni nanowire/cellulose hybrid structure. Japanese Journal of Applied Physics, 2018, 57, 02CA09.	1.5	2
201	Application of Anomalous X-ray Scattering Method to Liquid Electrolytes Used in a Battery: Local Structural Analysis around a Dilute Metallic Ion. Analytical Chemistry, 2020, 92, 9956-9962.	6.5	2
202	Current Views on the Structural Study of Interface of Liquids and Surface Layer of Solids ISIJ International, 1992, 32, 3-10.	1.4	1
203	Structural Study of Amorphous La(Co _{1−<1>x} TM<1> _x) ₁₃ Alloys by X-ray Diffraction. Materials Transactions, JIM, 1999, 40, 7-12.	0.9	1
204	Local Structure Change Around Ni Atoms in MgNi Alloys during Mechanical Alloying Process. Journal of Metastable and Nanocrystalline Materials, 2004, 20-21, 635-640.	0.1	1
205	In situ detection method for obtaining permeability of Fe-based amorphous alloys: ac resistance measurement for Fe84Nb7B9. Applied Physics Letters, 2005, 86, 032503.	3.3	1
206	Measurment of Incident Beam Angular Dependence of X-Ray Luminescence Intensity and Possibility of New Atom Resolved Holography. Bunseki Kagaku, 2006, 55, 441-446.	0.2	1
207	Elastic Properties of Cu-Based Bulk Metallic Glass around Glass Transition Temperature. Materials Science Forum, 2007, 539-543, 1932-1936.	0.3	1
208	Molecular Dynamics Simulation and Statistical Analysis for Glass Transition in a Lennard-Jones System. Nippon Kinzoku Gakkaishi/Journal of the Japan Institute of Metals, 2008, 72, 158-162.	0.4	1
209	Electrochemical Iron-Chromium Alloying of Carbon Steel Surface Using Alternating Pulsed Electrolysis. Materials Transactions, 2008, 49, 1346-1354.	1.2	1
210	Effects of Transformation Strain Due to Lithiation/delithiation in Sn Electrode of Li-ion Batteries. Electrochemistry, 2010, 78, 460-462.	1.4	1
211	An experimental procedure for precise evaluation of electron density distribution of a nanostructured material by coherent x-ray diffraction microscopy. Review of Scientific Instruments, 2010, 81, 033707.	1.3	1
212	Formation of Nickel Nanowires by Electroless Deposition. ECS Transactions, 2012, 41, 1-7.	0.5	1
213	Ingredients of the Soup in the Chemist's Cauldron: Structural Analysis of Organometallics in the Solution by X-ray Yuki Gosei Kagaku Kyokaishi/Journal of Synthetic Organic Chemistry, 2002, 60, 383-388.	0.1	1
214	Materials Science in Metallic Glasses. Zairyo/Journal of the Society of Materials Science, Japan, 2009, 58, 187-192.	0.2	1
215	Electrochemical Analysis in Fabrication of Co-Ni Alloy Nanoparticles in Nonaqueous Solution. Journal of MMIJ, 2011, 127, 103-107.	0.3	1
216	Characterization of the environmental structure of disordered materials using anomalous X-ray		1

scattering. , 1993, , 14-21.

#	Article	IF	CITATIONS
217	Frontiers in Crystallography with Synchrotron Radiation. X-ray Studies near Absorption Edges of Elements. Atom-Selective Experiments. Structure Analysis of Disordered Materials by the Anomalous X-ray Scattering(AXS) Method Nihon Kessho Gakkaishi, 1997, 39, 20-25.	0.0	1
218	Peculiar structure of X-ray standing wave lines of Si:As. Nuclear Instruments & Methods in Physics Research B, 2003, 199, 382-385.	1.4	0
219	Stability and Icosahedral Transformation of Supercooled Liquid in Metal-Metal type Bulk Glassy Alloys. Materials Research Society Symposia Proceedings, 2003, 805, 188.	0.1	Ο
220	Stability and Icosahedral Transformation of Supercooled Liquid in Metal-Metal type Bulk Glassy Alloys. Materials Research Society Symposia Proceedings, 2003, 806, 161.	0.1	0
221	Hydrogen Permeation Characteristics and Structural Features of Melt-Spun Ni-Nb-Zr Amorphous Alloy Membranes. Journal of Metastable and Nanocrystalline Materials, 2005, 24-25, 315-318.	0.1	Ο
222	Ultrasonic Spectroscopy and X-Ray Diffraction Study for ARB Aluminum. Materials Science Forum, 2007, 561-565, 937-940.	0.3	0
223	A Proposal for the New Concept of Structures of Metallic Glasses. Funtai Oyobi Fummatsu Yakin/Journal of the Japan Society of Powder and Powder Metallurgy, 2009, 56, 679-682.	0.2	Ο
224	Development of incident x-ray flux monitor for coherent x-ray diffraction microscopy. Journal of Physics: Conference Series, 2009, 186, 012060.	0.4	0
225	Nanostructure analysis by coherent hard X-ray diffraction. Journal of Physics: Conference Series, 2009, 186, 012056.	0.4	Ο
226	āfªāfā,¦āfā,ã,ªāf³è""é›»æ±ç"ç©¶ã«ãŠãʿã,‹é‡ʿ属朖™çµ"ç1"å¦çš"見æ–1. Keikinzoku/Journal of Japan Instit	ute∞afLigh	nt Moetals, 201
227	Formation of Columnar-Shaped Structure of Fe in Fe–Cr–Sn Thin Films and Its Shape-Magnetic Anisotropy. Japanese Journal of Applied Physics, 2011, 50, 013004.	1.5	0
228	A Possible Way of Utilizing a Polyvalent Metal As a Negative Electrode of Storage Battery. ECS Meeting Abstracts, 2013, , .	0.0	0
229	Formation of Cobalt Nanoparticles from Co(OH) ₂ Suspension. Advanced Materials Research, 0, 974, 50-54.	0.3	Ο
230	Electronic, Structural, and Electrochemical Modulation of Electrostatic Self-Assembled 1T-MoS ₂ Nanosheets via Topotactic Structural Conversion. E-Journal of Surface Science and Nanotechnology, 2015, 13, 1-7.	0.4	0
231	Framework Structures for Mg Battery Cathodes. Materials Science Forum, 2016, 879, 2150-2152.	0.3	Ο
232	Facile Synthesis of Ni Nanowire Composite via Liquid Phase Reduction: Effect of a Magnetic Field. Materials Science Forum, 0, 936, 20-24.	0.3	0
233	Li 2 NbO 3 –Li 2 MnO 3 Pseudoâ€Binary Compounds Crystallizing into Distorted Rocksalt Structures. Physica Status Solidi (B): Basic Research, 2019, 256, 1900003.	1.5	0
234	Three-dimensional Imaging of Nanoscale Internal Structure by Coherent X-ray Diffraction Microscope. Materia Japan, 2007, 46, 827-827.	0.1	0

#	Article	IF	CITATIONS
235	Local Structural Analyses of Non-crystalline Materials by the Anomalous X-ray Scattering(AXS) Method Nihon Kessho Gakkaishi, 1997, 39, 309-314.	0.0	0